

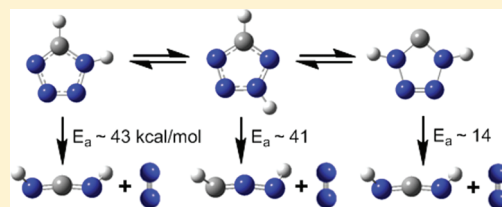
Tautomerism and Thermal Decomposition of Tetrazole: High-Level *ab Initio* Study

Vitaly G. Kiselev,* Pavel B. Cheblakov, and Nina P. Gritsan

Institute of Chemical Kinetics and Combustion, 3, Institutskaya Street, Novosibirsk, 630090 Russia, and Novosibirsk State University, 2, Pirogova Street, Novosibirsk, 630090 Russia

S Supporting Information

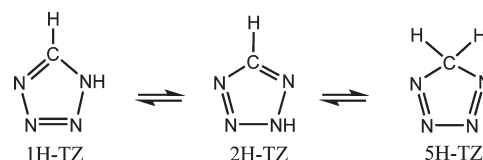
ABSTRACT: The mutual interconversion and decomposition reactions of four tetrazole isomers (1H-TZ, 2H-TZ, 5H-TZ, and an N-heterocyclic carbene 14H) have been studied theoretically using the W1 high-level procedure. Computations allowed resolution of the existing discrepancies in the mechanism and key intermediates of TZ thermolysis. The tautomeric equilibria between 1H-TZ, 2H-TZ, and 14H turned out to play a very important role in the mechanism of thermal decomposition. Although the barriers of monomolecular tautomeric transformations were found to be high (~ 50 – 70 kcal/mol), the concerted double H atom transfer reactions in the H-bonded complexes of TZ tautomers have profoundly lower barriers (~ 18 – 28 kcal/mol). These reactions lead to fast interconversion between 1H-TZ, 2H-TZ, and 14H. The carbene 14H has never been considered before; however, it was predicted to be a key intermediate in the mechanism of thermal decomposition of TZ. For all species considered, the unimolecular reactions of N_2 elimination were predicted to dominate over the elimination of hydrazoic acid. In agreement with existing experimental data, the effective activation energy of thermolysis was calculated to be 36.2 kcal/mol.

**INTRODUCTION**

Nitrogen-rich heterocycles and their derivatives have recently attracted considerable attention as promising environmentally friendly energetic compounds.^{1–6} Among them, tetrazole (TZ) is of significant interest for combustion chemistry^{7–9} due to its high heat of formation, thermal stability, and high nitrogen content. TZ is a widely used building block for a huge family of novel high-energy compounds.^{10–20} Apart from this, the electron-donating nitrogen atoms in the TZ ring can bind to various metal ions, forming stable complexes. For this reason, TZ and its derivatives are widely used as ligands in metal–organic chemistry.^{21–23} In addition, the acidities of TZ and its derivatives are similar to those of carboxylic acids, making them useful bioisosteres.^{24,25}

The annular tautomerism is very typical of tetrazole and its derivatives (Scheme 1).^{26–30} The tautomerism in tetrazoles has been studied in great detail both experimentally and theoretically for almost as long as there have been practical methods for synthesizing these species.^{26,27} Nevertheless, some issues concerning tautomeric equilibria in TZ still remain unclear. Moreover, even though the thermal decomposition of TZ under various conditions has also been intensively studied experimentally, there are still some contradictory assumptions concerning the initial reactions of its thermolysis.

The standard state of TZ is crystalline; its melting point is 156–157 °C.^{31–33} In the solid state, X-ray diffraction data undoubtedly indicate that TZ exists as a 1H form (1H-TZ, Scheme 1).³⁴ The comparison of dipole moments obtained from the microwave spectra of gaseous TZ and its deuterated analogues led the authors³⁵ to conclusion that both the 1H and 2H tautomers (Scheme 1) coexist in the gas phase. However, subsequent studies employing photoelectron³⁶

Scheme 1

and mass spectroscopies³⁷ indicated the predominance of the 2H form (2H-TZ) in the gas phase. The thorough calorimetric measurements of heat capacity of crystalline and gaseous TZ showed³³ that a sole tautomer dominates in the gas phase. Unfortunately, it still was impossible to identify whether it was 1H or 2H. Fausto et al.³⁸ performed matrix isolation of the TZ vapor at 10 K. Using IR spectroscopy along with quantum chemical calculations for vibrational spectra assignment, the authors concluded that the 2H form dominates in the vapor. From the estimated concentration ratio 2H:1H of ca. 9:1, the enthalpy difference between the tautomers at 363 K was suggested to be ~ 1.7 kcal/mol.³⁸

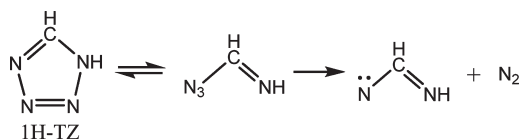
In polar solution, the solvent effect leads to shifting the tautomeric equilibrium to the more polar 1H form. On the basis of ¹H NMR studies and qualitative dipole moment considerations, 1H tautomer was supposed to dominate over the 2H form in DMF solution.³⁹ This suggestion was further supported by ¹³C NMR studies⁴⁰ for dioxane, DMSO, DMF, H₂O, and acetone as solvents

Received: December 30, 2010

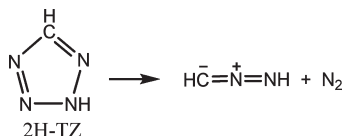
Revised: January 20, 2011

Published: February 15, 2011

Scheme 2



Scheme 3



and by ^{15}N NMR for *d*-chloroform and DMSO solutions.⁴¹ In all these solvents, the TZ exists almost exclusively in the 1H form.

Theoretical calculations at various reliable levels of theory confirmed that in the gas phase the 2H form is slightly more preferable thermodynamically than the 1H form. The formation enthalpy $\Delta_f H_{\text{gas}}^\circ$ of 2H-TZ was predicted to be ~ 1.5 – 2 kcal/mol lower than that of 1H-TZ.^{42,43} At the same time, quantum chemical computations (the PCM model was applied to take the solvation into account) showed that the polar 1H tautomer is more preferable than the 2H form in solutions with dielectric constant $\varepsilon \geq 7$.⁴⁴

Note that all above-mentioned studies dealt with the equilibrium of 1H and 2H tautomers of TZ. On the other hand, Wentrup et al.⁴² considered computationally another possible isomer: the 5H form (5H-TZ, Scheme 1). At the QCISD level of theory, 5H-TZ was found to be ~ 20 kcal/mol thermodynamically less favorable than 1H-TZ.⁴² The authors also found the activation barrier of unimolecular transformation 5H-TZ \rightarrow 1H-TZ to be significant (~ 36 kcal/mol) and therefore suggested 5H-TZ is a detectable species.⁴² However, to the best of our knowledge, 5H-tetrazole has never been observed experimentally.

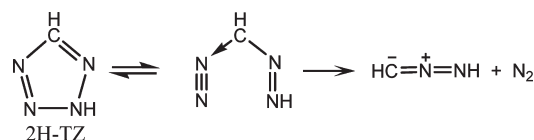
Lesnikovich et al.^{45–48} pointed out the importance of tautomeric transformations (Scheme 1) in the mechanism of TZ thermal decomposition. The authors found that the decomposition started at temperatures slightly higher than the melting point of the sample. TZ was proposed to exist in the 1H form in the melt. On the basis of differential scanning calorimetric (DSC) measurements, it was speculated that the thermal decomposition of the molten TZ occurred mainly through the open-ring azido form undergoing dissociation to N_2 and a corresponding nitrone (Scheme 2).⁴⁶

At the same time, the TZ was supposed to transform to 2H-TZ upon evaporation.⁴⁷ It was proposed that in the gas phase 2H-TZ decomposes via elimination of N_2 (Scheme 3).

The authors also investigated the final products of thermal decomposition of TZ in both the gas phase and melt using IR and mass spectroscopies.⁴⁷ Thermolysis of the molten TZ yielded N_2 , H_2 , and HCN among the most abundant gaseous products (apart from this, small amounts of HN_3 were also found), and an unidentified polymer was detected in the nonvolatile residue. Thermal decomposition of TZ in the gas phase led to N_2 , H_2 , and HCN; no other products were detected.⁴⁷

Lesnikovich et al.^{45,46} also derived the Arrhenius parameters of mass loss kinetics of the TZ sample using nonisothermal DSC data. However, the activation energy, preexponential factor, and even the effective reaction order were found to be strongly dependent on the experimental conditions⁴⁵ and, in particular, on

Scheme 4



the heating rate.⁴⁶ The activation energy and the preexponential factor calculated using different approaches varied from 36.5 to 42.6 kcal/mol and from $\log A \approx 14.4$ to $\log A \approx 17.3$, respectively.⁴⁵

In contrast to Lesnikovich et al., Ostrovskii et al.⁴⁹ proposed another mechanism of TZ thermolysis. Using the manometry technique, the authors measured the rate of gas evolution by a TZ sample under isothermal conditions. The thermal decomposition of TZ was studied in the gas phase and in the melt in the temperature range 180–230 °C, and in PhNO_2 solution at 150–190 °C.⁴⁹ The kinetics of the TZ thermolysis was described as a first-order process with similar values of activation energy, $E_a \approx 33$ kcal/mol, in both the gas phase and solution. A slightly higher value of $E_a \approx 37$ kcal/mol was found for the thermal decomposition in the melt. However, the preexponential factor varied from $\log A = 11.5$ in the gas phase to $\log A = 14.7$ in the melt in such a way that they almost completely compensated for the differences in the activation energies. For instance, the rate constant of the gas-phase decomposition of TZ at 190 °C was just 1.5 times lower than the rate constant in the melt.⁴⁹

Using the same experimental technique, the authors also studied the thermolysis of various TZ derivatives^{49,50} and hypothesized the initial reactions of TZ decomposition in accordance with Scheme 4. The 1H-tetrazole was supposed to be stable under experimental conditions, and a stepwise mechanism of the N_2 elimination was proposed for the decay of the 2H tautomer (Scheme 4).

Guimon et al.⁵¹ reported results of a flash vacuum pyrolysis (FVP) of the TZ at ~ 830 °C. The most intensive bands in the photoelectron spectra of gas products of FVP were attributed to cyanamide (NH_2CN), HCN, N_2 , and diazomethane (CH_2N_2). On the basis of experimental results and quantum chemical calculations at semiempirical and Hartree–Fock levels, the authors⁵¹ proposed the intermediacy of diaziridine, a three-member cyclic compound, in the decomposition of TZ.

Maier et al.⁵² performed similar FVP experiments at 800 °C with a subsequent matrix isolation of the products of pyrolysis. In contrast to the results of Guimon et al.,⁵¹ the main products detected by IR spectroscopy were HCN and HN_3 ; other weaker IR bands were attributed to NH_2CN , CH_2N_2 , carbodiimide ($\text{HN}=\text{C}=\text{NH}$), and nitrilimine ($\text{HC}=\text{N}=\text{NH}$).

Sinditskii et al.⁵³ performed a thermocouple study of TZ combustion. The maximum temperature in the flame varied with the external pressure from 1065 to 1225 °C. The final products of combustion HCN, H_2 , and N_2 were proposed to match the measured burning surface temperature. These findings agree well with the results of Lesnikovich et al.⁸ The authors analyzed the products of TZ combustion using mass spectrometry and found HCN, H_2 , and N_2 to be the most abundant ones.

Kawaguchi et al.⁵⁴ reported results of T-jump/FTIR experiments in a wide range of heating rates (from 1 to 1000 K/s). The authors detected HCN, HN_3 , C_2H_2 , and CH_4 among the decomposition products and proposed the decomposition to $\text{HCN} + \text{HN}_3$ to be the primary reaction of thermolysis of TZ.

This conclusion seems to be very doubtful as the concentration of the IR inactive N_2 was not monitored at all.

Thermodynamic characteristics of TZ and intermediates of its thermal decomposition and the rate constants of elementary reactions are crucial for modeling the complex process of thermolysis. However, it is seen that the existing experimental data on the primary reactions of the TZ thermal decomposition are incomplete and contradictory.^{45–47,49,51} Moreover, since the distribution of the primary reaction products cannot be measured directly and the information about tautomeric equilibrium of TZ (Scheme 1) is lacking, the proposed mechanisms (Schemes 2–4) are to some extent speculative. A number of different pathways and key intermediates of the TZ thermolysis have been proposed so far, but they have not been supported and substantiated with sufficient experimental evidence. Moreover, the existing estimations of the activation barriers and rate constants of the elementary reactions are based exclusively either on the nonisothermal kinetics of a sample weight loss^{45,46} or on the rate of the sample gas evolution.⁴⁹ Unfortunately, the results from thermogravimetry experiments can be subject to factors that are not directly related to reaction kinetics, such as mass- and heat-transfer limitations, evaporation, and the accuracy of the model used to calculate these parameters. In reactions of complex solid systems, separating these artifacts from the intrinsic reaction kinetics is often impossible.

The problems in the measurement of the elementary reaction rate constants are mainly due to a significant number of fast simultaneous processes in the melt and gas phase with numerous short-lived intermediates involved. The experimental difficulties in the detection of some intermediates and products (e.g., IR-inactive molecular nitrogen) are a serious obstacle. Moreover, the kinetic measurements are hindered by nonisothermal experimental conditions (e.g., the final product distribution depends on the heating rate).^{45,46}

Quantum chemical calculations are the most appropriate alternative for the study of the elementary reactions of TZ thermolysis. In a very recent paper, da Silva and Bozzelli⁵⁵ considered the gas-phase primary reactions of thermal decomposition of 1H- and 2H-TZ using the G3B3 multilevel procedure. The N_2 elimination reaction was predicted to dominate for both 1H- and 2H-TZ isomers, and the effective activation energy of TZ decomposition (the sum of all reaction channels was considered) in the temperature range 300–2000 K was found to be 37.2 kcal/mol.

However, to the best of our knowledge, the reactions of 5H-TZ and other possible tautomers of TZ have never been analyzed. Moreover, the bimolecular reactions of TZ have never been considered in the literature.

The main goals of our paper are to investigate theoretically the thermodynamic properties of different possible isomers of TZ, to identify clearly the intermediates of their primary reactions, and, eventually, to give insight into the mechanism of primary stages of the TZ thermal decomposition. The solid-state decomposition was found experimentally to be negligible for TZ; thermolysis proceeds in the melt and gas phase.^{45,46} Therefore, we calculated the activation barriers of the primary reactions in the gas phase. In contrast to all previous publications, we also considered the bimolecular reactions of TZ and demonstrated their importance.

COMPUTATIONAL DETAILS

To obtain reliable values of activation barriers and reaction enthalpies, we employed the highly accurate W1 composite procedure.⁵⁶ Although this technique was initially designed for

accurate computations of thermodynamic values (atomization energy/formation enthalpy, ionization potentials, etc.) rather than kinetics (localization of transition states and calculations of activation barriers), it is indeed a well-defined robust method of the approximate all-electron CCSD(T)/CBS (extrapolated to a complete basis set) quality. Therefore, we opted for the W1 technique to consider the unimolecular reactions of TZ thermolysis. Note that the moderate size of this system renders W1 feasible in the present case. The Gaussian implementation W1Usc (UCCSD(T) instead of ROCCSD(T) along with a small spin contamination correction)^{57,58} of the W1 method was employed for open-shell species.

The G3B3 multilevel technique⁵⁹ has been applied for the study of the bimolecular reactions of various TZ isomers. All the equilibrium and transition state structures were ascertained to be the minima and saddle points, accordingly, on the potential energy surfaces (PES). The corresponding thermal corrections were included in order to obtain the enthalpy and Gibbs free energy values at the desirable temperature. The gas-phase enthalpies of formation (at $p = 1$ atm and $T = 298.15$ K, $\Delta_f H_{\text{gas}}^\circ$) were obtained using the atomization energy approach described elsewhere.⁶⁰ The heats of formation at 0 K for the elements in the gas phase $\Delta_f H_{\text{gas}}^{0\text{K}}(\text{C}) = 169.98$ kcal/mol, $\Delta_f H_{\text{gas}}^{0\text{K}}(\text{H}) = 51.63$ kcal/mol, $\Delta_f H_{\text{gas}}^{0\text{K}}(\text{N}) = 112.53$ kcal/mol were taken from the NIST-JANAF tables.⁶¹

The thermal corrections ($H_{298\text{K}} - H_{0\text{K}}$) for the most part of the species studied were obtained using the rigid rotor–harmonic oscillator approximation. Some methyl-substituted derivatives of TZ possess low-frequency vibrational modes corresponding to hindered rotations of the CH_3 group. The appropriate corrections to partition functions in this case were made using the Pitzer–Gwinn approach⁶² implemented in Gaussian 09.⁶³

The role of multireference character in the wave functions of the reagents, intermediates, and transition states considered in the present work was estimated using the T1 diagnostic for the CCSD calculation.⁶⁴ Modest T1 values obtained in all cases (<0.03) indicate that a single reference-based electron correlation procedure is appropriate in the present case.

All quantum chemical computations, except otherwise noted, were performed using the Gaussian 09 suite of programs.⁶³

The rate constants of monomolecular reactions in the gas phase at a high pressure limit were computed in accordance with the canonical transition state theory (TST):

$$k(T) = \alpha \frac{kT}{h} \exp\left(-\frac{\Delta G^\ddagger(T)}{kT}\right) \quad (1)$$

where α is a statistical factor (a number of equivalent reaction channels); ΔG^\ddagger is a free energy of activation calculated using the W1 electronic energy and corresponding thermal corrections. The TST rate constants were calculated in the temperature range 450–750 K with a step of 150 K and then approximated by the Arrhenius equation:

$$k = A \exp(-E_a/RT) \quad (2)$$

RESULTS

Formation Enthalpies of Various Isomeric Forms and Derivatives of TZ. The properties of seven different isomeric forms of TZ have been studied (Chart 1). Apart from the 1H, 2H, and 5H tautomers of TZ discussed before (Scheme 1), we considered another possible isomer of TZ, 23H, and several N-heterocyclic carbenes (14H, 13H, and 12H; Chart 1) as well.

Chart 1

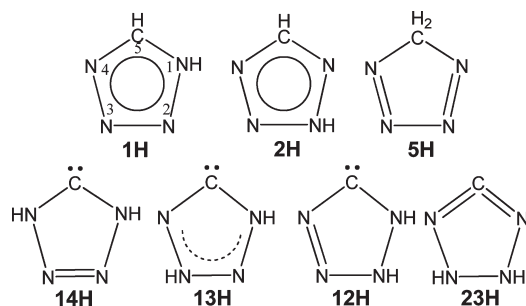


Table 1. Relative Gas-Phase Enthalpies at 0 K ($\Delta(\Delta H_{\text{gas}}^{0\text{K}})$) of Various Isomers of TZ^a and Their Gas Phase Formation Enthalpies at 0 K ($\Delta_f H_{\text{gas}}^{0\text{K}}$) and 298 K ($\Delta_f H_{\text{gas}}^\circ$) Calculated at the W1 Level of Theory (All Values in kcal/mol)

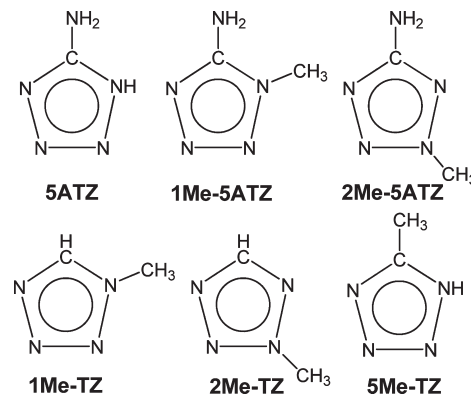
compound	$\Delta(\Delta H_{\text{gas}}^{0\text{K}})^a$	$\Delta_f H_{\text{gas}}^{0\text{K}}$	$\Delta_f H_{\text{gas}}^\circ$	$\Delta_f H_{\text{gas}}^\circ$, expt
1H-TZ	0.0	82.7	79.1 80.2 ^b 81.0 ^c 82.3 ^d	78.1 ^e
2H-TZ	-1.7	81.0	77.3 79.0 ^c 80.4 ^d	
5H-TZ	22.9	105.6	102.5	
14H	20.5	103.2	99.6	
13H	40.4	123.1	119.4	
12H	53.5	136.2	133.0	
23H	71.5	154.2	150.8	
5-ATZ		82.5	77.7 81.5 ^d	77.5 ^f
1-Me-5-ATZ		79.1	73.1 76.6 ^d	72.3 ^g 74.9 ^h
2-Me-5-ATZ		75.3	69.2 72.3 ^d	71.4 ^g 72.4 ^h
1-Me-TZ		79.7	74.7	77.2 ^g
2-Me-TZ		76.3	71.2	78.5 ⁱ
5-Me-TZ		72.3	67.4	67.1 ^g

^a 1H-TZ was chosen as a reference species for computations of the relative thermodynamic properties. ^b CCSD(T)/CBS value, ref 71. ^c A weighted average of G3, G3B3, and CBS-APNO values, ref 72. ^d G3 value, ref 73. ^e The most reliable experimental result, ref 33 (cf. discussion in the text). ^f A sum of $\Delta_f H_{\text{solid}}^\circ$ from ref 65 and $\Delta_{\text{sub}} H^\circ$ from ref 32. ^g A sum of $\Delta_f H_{\text{solid}}^\circ$ and $\Delta_{\text{sub}} H^\circ$ from ref 32. ^h A sum of $\Delta_f H_{\text{solid}}^\circ$ from ref 70 and $\Delta_{\text{sub}} H^\circ$ from ref 32. ⁱ A sum of $\Delta_f H_{\text{liquid}}^\circ$ and $\Delta_{\text{vap}} H^\circ$ from ref 32.

The calculated gas-phase formation enthalpies at 0 K ($\Delta_f H_{\text{gas}}^{0\text{K}}$) and 298 K ($\Delta_f H_{\text{gas}}^\circ$), the relative enthalpies at 0 K of the various isomers of TZ are listed in Table 1. Some results of other high-level calculations available in the literature are also included for the sake of comparison. In addition, we calculated $\Delta_f H_{\text{gas}}^\circ$ values of some tetrazole derivatives (Table 1), viz., 5-aminotetrazole (5-ATZ) and several methyl-substituted analogues of TZ and 5-ATZ (Chart 2).

Unfortunately, the existing experimental thermochemical data on TZ and its derivatives are rather scarce and sometimes contradictory. Moreover, since the standard state of all these compounds is

Chart 2



crystalline, the gas-phase formation enthalpies listed are actually the sum of two independently measured experimental values: the solid state heat of formation $\Delta_f H_{\text{solid}}^\circ$ and the sublimation enthalpy $\Delta_{\text{sub}} H^\circ$.

We would like to emphasize the existing discrepancy among the experimental values of $\Delta_f H_{\text{gas}}^\circ$ for 1H-TZ. The value of $\Delta_f H_{\text{solid}}^\circ$ for TZ (56.66 kcal/mol) was obtained by McEwan and Rigg using static bomb calorimetry and reported in 1951.⁶⁵ In the same article, the authors also reported⁶⁵ the sublimation enthalpy of TZ, $\Delta_{\text{sub}} H^\circ = 23.26$ kcal/mol. However, this value was based on a private communication and no experimental details were available.⁶⁵ The resulting gas-phase formation enthalpy $\Delta_f H_{\text{gas}}^\circ = \Delta_f H_{\text{solid}}^\circ + \Delta_{\text{sub}} H^\circ = 79.9$ kcal/mol is listed, for instance, in the well-known compendium of Pedley.⁶⁶

The combustion experiments and vapor pressure measurements were repeated in the USSR in the 1970s.⁶⁷ The authors⁶⁷ found $\Delta_f H_{\text{solid}}^\circ = 56.4$ kcal/mol in perfect agreement with McEwan and Rigg.⁶⁵ At the same time, a remarkably different value of sublimation enthalpy was obtained ($\Delta_{\text{sub}} H^\circ = 20.2$ kcal/mol). Unfortunately, these results were reported only in a very local and difficult-to-access Russian book series.⁶⁷ Nevertheless, the corresponding value $\Delta_f H_{\text{gas}}^\circ = 76.7$ kcal/mol is given in the NIST Chemistry webbook.⁶⁸

At the beginning of the 1990s, the sublimation enthalpy of TZ was remeasured and the value $\Delta_{\text{sub}} H^\circ = 21.5$ kcal/mol was obtained.³² The latter quantity was confirmed independently shortly afterward by the use of another experimental technique (namely, differential heat-conduction microcalorimetry), and the final result of $\Delta_{\text{sub}} H^\circ = 21.4$ kcal/mol was derived.³³ Therefore, we believe the value $\Delta_f H_{\text{gas}}^\circ = 78.1$ kcal/mol to be the most reliable among the existing ones.

This issue clearly points out that experimental thermochemical data, even from the well-respected compilations, should not be considered (as often happens) as “no-questions-asked” exact benchmark values when testing the performance of various computational procedures. We have already faced similar issues dealing with the thermochemistry of nitroalkanes.⁶⁹ Attention should always be paid to the critical evaluation of primary literature sources.

The 5-ATZ case is reminiscent of the one discussed above. The formation enthalpy of the solid 5-ATZ ($\Delta_f H_{\text{solid}}^\circ = 49.7$ kcal/mol) was also reported by McEwan and Rigg.⁶⁵ Later the sublimation enthalpy was determined ($\Delta_{\text{sub}} H^\circ = 27.8$ kcal/mol) and the gas-phase formation enthalpy was finally obtained to be $\Delta_f H_{\text{gas}}^\circ = 77.5$ kcal/mol.³² Both $\Delta_f H_{\text{solid}}^\circ$ and $\Delta_{\text{sub}} H^\circ$ values have been reported only one time.

Two generally accepted experimental values of $\Delta_f H_{\text{gas}}^\circ$ exist for 1-Me-5-ATZ and 2-Me-5-ATZ. Williams et al.⁷⁰ reported the

formation enthalpies of these species in the standard (crystalline) state, and later another group³² reassessed these values and measured the sublimation enthalpy as well (Table 1). It is hard to conclude which of the two quantities is more reliable in this case.

The authors³² also obtained the $\Delta_f H_{\text{gas}}^\circ$ values for 1-Me-TZ, 5-Me-TZ (crystalline under normal conditions), and 2-Me-ATZ (standard state, liquid). Again, the formation enthalpies of these species in the standard state were combined with the sublimation and vaporization enthalpies, respectively³² (Table 1). Note that the 2-Me isomer was found to be slightly less stable thermodynamically than the 1-Me one (Table 1).

It is seen from Table 1 that the experimental value of $\Delta_f H_{\text{gas}}^\circ$ for TZ lies between the W1 predictions for 1H-TZ and 2H-TZ. It is also instructive to compare the W1 results with other computations at various high levels of theory (Table 1). The G3 value⁷³ and a weighted average of G3, G3B3, and CBS-APNO values⁷² turn out to be higher than the W1 one by ~ 3 and 2 kcal/mol, respectively (Table 1). The W1 is generally a more accurate composite procedure than the latter methods, and it is reasonable to expect the W1 formation enthalpy of 1H-TZ $\Delta_f H_{\text{gas}}^\circ = 79.1$ kcal/mol to be more robust. However, the value $\Delta_f H_{\text{gas}}^\circ = 80.2$ kcal/mol has been calculated⁷¹ at the CCSD(T)/CBS level of approximately the same quality as the W1. A detailed inspection of the W1 and CCSD(T)/CBS results⁷¹ shows that the difference of about 1 kcal/mol originates from the inner-shell correlation and scalar relativistic correction to the total atomization energies. While in the W1 procedure these corrections are both accounted for at the CCSD(T)/MTSmall level using the Douglas–Kroll–Hess Hamiltonian,⁵⁶ the authors⁷¹ applied the MP2/cc-pVTZ method with the same Hamiltonian for relativistic corrections and CCSD(T)/cc-pwCVTZ for core–valence contribution. As the basis sets used are of comparable size, the W1 value seems to be more reliable. It is also worth mentioning that the “bare” energy difference of 2.07 kcal/mol (ZPE excluded) between the 2H-TZ and 1H-TZ recently calculated using the very accurate focal-point analysis technique⁴³ is in perfect agreement with the value 2.1 kcal/mol predicted by the W1.

Table 1 also shows that the W1 prediction for 5-ATZ ($\Delta_f H_{\text{gas}}^\circ = 77.7$ kcal/mol) is in very good agreement with experiment. The W1 values of $\Delta_f H_{\text{gas}}^\circ$ of 1-Me-5-ATZ agree well with the result of the earlier experiment.⁶⁵ However, in the case of 2-Me-5-ATZ the discrepancy is about 2 kcal/mol (Table 1).

The most pronounced contradiction between theory and experiment occurs in the case of methyl derivatives of TZ (Table 1). While 1-Me-TZ was experimentally predicted to be slightly more stable thermodynamically than 2-Me-TZ, computations put the 2-Me isomer at ~ 3.5 kcal/mol below 1-Me-TZ (Table 1). Moreover, the formation enthalpies of these species also differ remarkably from the experimental values. The W1 value of $\Delta_f H_{\text{gas}}^\circ$ of 2-Me-TZ is 7.3 kcal/mol lower than the experimental one (Table 1). Taking into account that the computations predict the same order of isomers (the enthalpies of 1-Me species are higher than those of 2-Me) in the case of aminotetrazole derivatives (see above), we beg to differ with the authors³² on these important thermochemical parameters. At the same time, in the case of 5-Me-TZ the agreement between the experiment and theory is perfect (Table 1). The possible origin of experimental data inconsistency for the 2-Me-TZ species might be the phase transition (the melting point of this compound is ca. 15 °C)³² which complicates the vapor pressure measurements.

In general, the results obtained show that the $\Delta_f H_{\text{gas}}^\circ$ values of the different tautomers and derivatives of TZ at the W1 level are ~ 3 –4 kcal/mol lower than their G3 counterparts (Table 1).

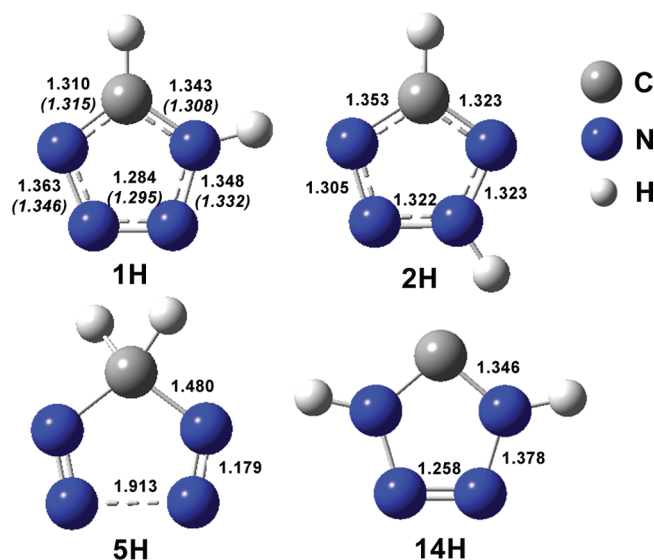


Figure 1. Geometries (bond lengths in Å) of the different isomers of TZ optimized at the B3LYP/cc-pVTZ level (experimental bond lengths³⁴ are given in parentheses).

Note, however, that the enthalpy differences (e.g., between 1H-TZ and 2H-TZ or 1-Me-5-ATZ and 2-Me-5-ATZ) are reproduced well by both methods (Table 1). We believe the W1 gas-phase formation enthalpies presented here to be the most reliable estimations for the species considered.

Although 2H-tetrazole is predicted to be the most stable gas-phase isomer, the enthalpy difference between 2H-TZ and 1H-TZ is rather small (1.7 kcal/mol at 0 K Table 1). The 5H form, due to the lack of aromaticity in the tetrazole ring, is predicted to be significantly less favorable than 2H and 1H (by ~ 23 kcal/mol, Table 1). Note that another isomer of TZ, the N-heterocyclic carbene 14H (Chart 1), is even slightly more favorable than 5H (Table 1). The ground state of 14H-TZ is singlet, the singlet–triplet (ST) splitting (ΔE_{ST}) is predicted to be large ($\Delta E_{\text{ST}} = -92.5$ kcal/mol) at the W1 level. Note that similar values of ΔE_{ST} (-61 to -84 kcal/mol) were reported for a series of N-heterocyclic carbenes.⁷⁴ The relative formation enthalpies of other possible isomers (13H, 12H, and 23H, Chart 1) are considerably higher than those of the former species. Therefore, we concentrated our efforts on the detailed study of the four isomers marked in boldface type in Table 1.

Geometries of TZ Isomers. Figure 1 represents geometries of the 1H, 2H, 5H, and 14H isomers optimized at the B3LYP/cc-pVTZ level (in the framework of the W1 procedure). The full structural descriptions of all studied species are available in the Supporting Information.

The tetrazole ring was found to be planar for all species considered (Figure 1). The experimental crystallographic data exist only for the α -polymorph of 1H-TZ.³⁴ It is seen from Figure 1 that the theoretical and experimental bond lengths coincide fairly well (within 0.015 Å), with the only exception the C–N₁ bond (see Chart 1 for atomic labels). In this case the theoretical value is about 0.035 Å longer than the experimental one. Note, however, that the authors³⁴ found TZ molecules to be subjected to high-amplitude libration motions, and they proposed a corresponding correction to the observed bond lengths.³⁴ The corrected value of 1.327 Å deviates from the theoretical prediction by an acceptable 0.015 Å. Moreover, the

Table 2. Bond Lengths (Å) in the 5H-TZ Tautomer Optimized at Various Post-HF and DFT Levels of Theory

method	$r(\text{N}_2-\text{N}_3)$	$r(\text{C}-\text{N}_1)$	$r(\text{N}_1-\text{N}_2)$
MP2/aug-cc-pVTZ ^a	2.184	1.493	1.180
MP2/aug-cc-pVQZ	2.175	1.490	1.180
MP3/cc-pVDZ	1.606	1.466	1.222
MP4/cc-pVDZ	2.050	1.499	1.208
QCISD/6-31G(d) ^b	1.645	1.469	1.225
QCISD/aug-cc-pVTZ	1.619	1.462	1.214
QCISD(T)/cc-pVDZ	1.896	1.491	1.209
CCSD/cc-pVDZ	1.655	1.472	1.222
CCSD(T)/cc-pVDZ	1.897	1.491	1.208
CCSD(T)/aug-cc-pVTZ	1.839	1.479	1.200
B3LYP/cc-pVTZ	1.913	1.480	1.179
M06/6-311++G(3df,2p)	1.777	1.463	1.187
M06-2X/6-311++G(3df,2p)	1.589	1.455	1.207

^a Reference 43. ^b Reference 42.

molecular geometry obtained experimentally in the crystalline phase should not be necessarily identical to the gas-phase one.

A very interesting issue is the structure of the 5H tautomer (Figure 1). Although it would be natural to anticipate the cyclic geometry of this species (Chart 1), the B3LYP/cc-pVTZ optimization yields the N_2-N_3 bond to be unexpectedly long (1.91 Å, Figure 1). Note that Wentrup et al.⁴² optimized the geometry of this species at various correlated levels of theory. MP2 with different basis sets (up to 6-311+G(2d,2p)) predicted an open structure (N_2-N_3 bond length was ~ 2.6 Å).⁴² A recent optimization at the MP2/aug-cc-pVTZ level yielded the N_2-N_3 bond to be ~ 2.2 Å.⁴³ In the meantime, the cyclic structure of 5H-TZ has been optimized at the QCISD/6-31G(d) and MP3/6-31G(d) levels (the N_2-N_3 bond length was $\sim 1.5-1.6$ Å).⁴²

We optimized the geometry of 5H-TZ at several ab initio and DFT levels of theory (Table 2). All methods predict similar C– N_1 ($\sim 1.46-1.49$ Å, see Chart 1 for atomic labels) and N_1-N_2 ($\sim 1.18-1.22$ Å) bond lengths. These values are close, respectively, to a typical single C–N bond (e.g., 1.471 Å in methylamine, CH_3NH_2)⁷⁵ and a double N=N bond (1.247 Å in diazene, $\text{HN}=\text{NH}$).⁷⁶ At the same time, the N_2-N_3 bond length varies noticeably with the optimization method employed: from ~ 2.2 Å (MP2) to ~ 1.6 Å (M06-2X DFT functional).

It is seen from Table 2 that MP2 tends to overestimate the N_2-N_3 bond length: $r(\text{N}_2-\text{N}_3) = 2.175$ Å at the MP2/aug-cc-pVQZ level. MP3/cc-pVDZ tremendously decreases this value to 1.606 Å and MP4/cc-pVDZ level lengthens this bond back to 2.050 Å (Table 2). QCISD with a sufficiently large basis set (aug-cc-pVTZ) predicts cyclic structure ($r(\text{N}_2-\text{N}_3) = 1.619$ Å), while the perturbative inclusion of triple excitations (QCISD(T)/cc-pVDZ) gives ~ 1.90 Å. This tendency remains the same for the coupled cluster method. The highest level of theory feasible in the present case was CCSD(T)/aug-cc-pVTZ yielding $r(\text{N}_2-\text{N}_3) = 1.839$ Å (Table 2, values in boldface type).

Note also that for hybrid DFT functionals employed (B3LYP, M06, and M06-2X), an increase of the percentage of exact exchange leads to tightening of the N_2-N_3 bond (Table 2). The B3LYP/cc-pVTZ geometry (used in the WI procedure) is in reasonable agreement with the benchmark CCSD(T)/aug-cc-pVTZ one (the discrepancy does not exceed 0.1 Å, Table 2).

Nevertheless, the CCSD(T)/aug-cc-pVTZ value $r(\text{N}_2-\text{N}_3) = 1.839$ Å is remarkably higher than a typical single N–N bond length

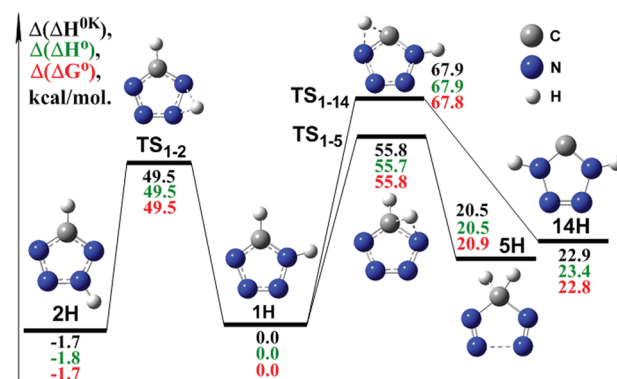


Figure 2. Stationary points on the PES of TZ corresponding to monomolecular interconversion of 1H, 2H, 5H, and 14H isomers. The 1H form is a reference compound for the calculations of the relative thermodynamic properties. All values are calculated at the W1 level and are given in kcal/mol.

(e.g., 1.447 Å in hydrazine, H_2NNH_2).⁷⁷ To get deeper insight into the nature of this bonding, QTAIM analysis^{78,79} has been performed using the B3LYP geometry and electron density of 5H-TZ. The N_2-N_3 bond critical point (BCP) was localized and found to have ρ_b and $\nabla^2\rho_b$ values, respectively, of 0.09 and 0.14 au. These values are not typical of covalent bonds ($\rho_b > 0.20$ and negative $\nabla^2\rho_b$ value).⁷⁹ The positive value of $\nabla^2\rho$ usually means closed-shell bonding, for example, hydrogen bonding or van der Waals interactions.⁷⁹ The absolute value of ρ in the BCP (0.09 au) is ca. 3 times lower than the one in hydrazine (0.30 au) and is the indication of very weak bonding. However, natural bond orbital (NBO) analysis⁸⁰ reveals that the highest occupied NBO of 5H-TZ is the N_2-N_3 σ bonding orbital, and the lowest unoccupied one is the N_2-N_3 σ^* antibonding one. This fact corresponds to a very weak covalent N_2-N_3 bonding.

Our calculations suggest that geometry optimization of 5H-TZ species requires unusually high correlated levels of theory with sufficient basis sets (such as CCSD(T)/aug-cc-pVTZ) to arrive at a reasonable final structure. However, the conventional B3LYP technique (rather incidentally, though) also yields very reasonable geometry.

Mutual Interconversion of TZ Isomers. As a next step in the study of tautomerism of TZ, we scrutinized the mutual transformations of the four above-mentioned isomers of TZ. Figure 2 demonstrates the stationary points on the PES for the monomolecular interconversion between the 1H, 2H, and 5H tautomers and the carbene 14H. The activation barriers for all monomolecular isomerization reactions are predicted to be very high (the lowest one corresponding to $1\text{H-TZ} \rightarrow 2\text{H-TZ}$ transformation is ~ 50 kcal/mol, Figure 2).

However, it is clear that TZ in all isomeric forms should be prone to forming hydrogen-bonded complexes. For instance, the X-ray diffraction studies of the crystalline structure of TZ revealed that the 1H-tetrazole molecules are linked by $\text{N}-\text{H}\cdots\text{N}$ and $\text{C}-\text{H}\cdots\text{N}$ bridges.³⁴ Therefore, we considered possible H-bonded complexes of the TZ tautomers of the lowest energy (viz., 1H and 2H). Figure 3 demonstrates the structures and relative energies of various H-bonded dimers formed by, respectively, two 1H-TZ molecules (D11) and two 2H-TZ molecules (D22) and of the complexes formed by a pair of 1H and 2H species (D12). Several H-bonding patterns might exist for a given pair of molecules (e.g., D22a and D22b, Figure 3). Note that the formation enthalpies of D12, D22, and D11a are quite close (within 2.5 kcal/mol) to each other.

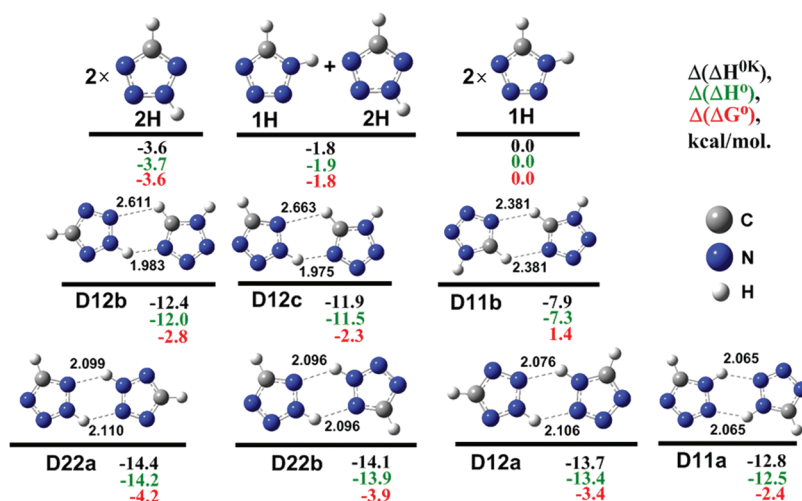


Figure 3. G3B3 relative enthalpies at 0 K ($\Delta(\Delta H^{0K})$, black numbers), relative enthalpies ($\Delta(\Delta H^\circ)$, green numbers), and Gibbs free energies ($\Delta(\Delta G^\circ)$, red numbers) at 298 K of the hydrogen-bonded dimers of 1H-TZ and 2H-TZ. Two separate monomers of 1H-TZ were chosen as a reference for relative thermodynamic properties. All energy values are given in kcal/mol, and N \cdots H hydrogen-bond lengths are in Å.

Figure 3 demonstrates also that concerted double hydrogen transfer in the H-bonded complexes might lead to interconversion of different TZ tautomeric forms. The H-transfer in the complexes shown in the third row of Figure 3 leads to transformations (in both directions) between 1H and 2H tautomers of TZ (e.g., D11a turns into D22b, D22a turns into D12a, etc.). Figure 4 (upper row) displays the stationary points for one example of such transformations with a lowest activation barrier. Even more fascinating is double H-transfer in the dimers from the second row of Figure 3. The products of these reactions are complexes of carbene 14H with either 1H or 2H species (Figure 4, bottom row).

As mentioned before, there are several possible ways to transform 1H-TZ to 2H-TZ in various H-bonded complexes (cf. the third row in Figure 3) and 1H-TZ to 14H as well (Figure 3, second row). Figure 4 displays the stationary points for the reactions with the lowest activation barriers among the considered complexes (Figure 3). It is seen that the barrier of 1H–2H isomerization (D11a \rightarrow D22b) is about 17 kcal/mol (cf. 49.5 kcal/mol in the corresponding monomolecular reaction, Figure 2). The second reaction, D12b \rightarrow D1-14, transforms 1H-TZ to 14H-TZ. Though the barrier of this process is about 27 kcal/mol (Figure 4), it is indeed noticeably lower than that of the monomolecular reaction (\sim 68 kcal/mol, Figure 2).

So far we have not considered the concerted double H-transfer reactions leading to the complexes of the 5H tautomer. Note that in all above-discussed structures the carbon atom is sp^2 hybridized and the monomers and H-bonded dimers are planar. On the other hand, the 5H form is not planar: the C atom is in the sp^3 hybridization state (Figure 1). Due to this fact, the C–N₄ rings in the complex formed by two 5H-TZ molecules are not coplanar, and this dimer turned out to be weakly bound (the enthalpy of complex formation is $\Delta(\Delta H^\circ) = -3.9$ kcal/mol, cf. Figure 3). Moreover, we were unable to localize any transition states corresponding to a conversion between 5H and other TZ tautomers. Nevertheless, the possibility of such processes cannot be entirely excluded.

It is clear that the concerted double hydrogen atom transfer in the H-bonded complexes plays an especially important role in the melt. However, it is obvious that the real structure of the melt and processes taking place upon melting are profoundly more complicated and could hardly be reduced to several simple reactions considered above.

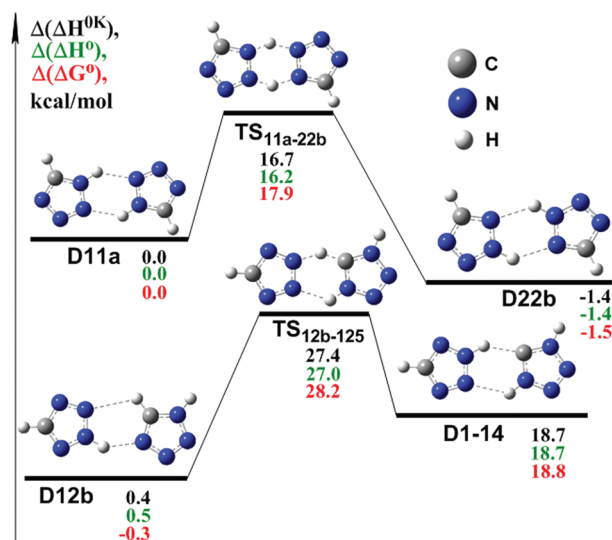


Figure 4. G3B3 relative enthalpies at 0 K ($\Delta(\Delta H^{0K})$, black numbers), relative enthalpies ($\Delta(\Delta H^\circ)$, green numbers), and Gibbs free energies ($\Delta(\Delta G^\circ)$, red numbers) at 298 K of the stationary points on the PES corresponding to mutual transformations of some H-bonded dimers of TZ. The dimer of the 1H forms (D11a) was chosen as a reference species for the calculations of the relative thermodynamic properties. All values are calculated at the G3B3 level of theory and are given in kcal/mol.

Nevertheless, it is obvious from the above-described consideration that the interconversion of different isomers of TZ through the bimolecular H-transfer reactions have noticeably lower barriers than the monomolecular ones in both the melt and gas phase. These processes might be of particular importance in the thermolysis of TZ. If the bimolecular interconversion reactions are significantly faster than the thermal decomposition reactions of monomers, the equilibrium between several TZ tautomers is maintained during the thermolysis of TZ. In this case, the thermal decomposition through the intermediacy of even thermodynamically unfavorable isomers (e.g., 5H-TZ and 14H-TZ) would contribute noticeably to the total rate of the TZ decay. Therefore, we consider next the barriers and the rate constants of the thermal decomposition of various TZ isomers.

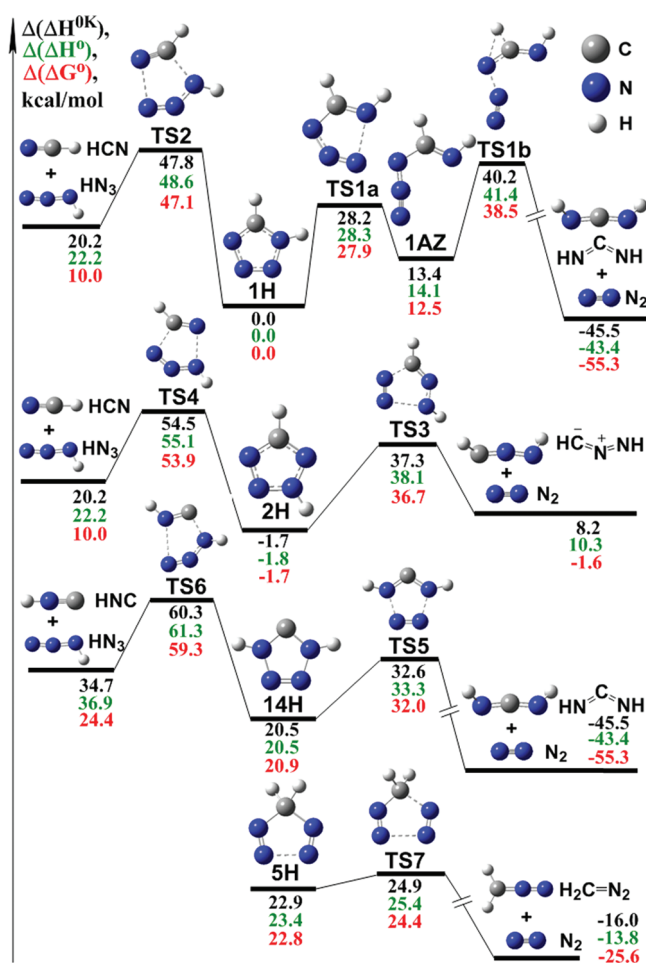


Figure 5. Relative thermodynamic parameters of the stationary points on the PES corresponding to thermal decomposition of 1H, 2H, 5H, and 14H tetrazole isomers. The 1H form was chosen as a reference compound for the calculations of the relative thermodynamic properties. All values are in kcal/mol and are calculated at the W1 level of theory.

Monomolecular Reactions of Thermal Decomposition of TZ Isomers. The stationary points on the PES corresponding to the lowest unimolecular decomposition channels of 1H, 2H, 5H, and 14H isomers are shown in Figure 5. For all species, except 5H, the two competing primary reactions are the eliminations of HN_3 (Figure 5, left side) and N_2 (Figure 5, right side), respectively. The most kinetically preferable monomolecular decomposition reactions of all isomers studied lead to the formation of N_2 (Figure 5 and Table 3, rate constants $k_{1\text{eff}}$, k_3 , etc.); the elimination of HN_3 is profoundly slower for all TZ isomers (Figure 5 and Table 3, rate constants k_2 , k_4 , and k_6).

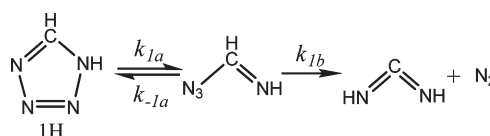
Using the Gibbs free energies of activation depicted in Figure 5, we calculated the rate constants of the elementary reactions in the temperature range 450–750 K using the TST theory (formula 1). The results were approximated by the Arrhenius equation (2), and the calculated Arrhenius parameters are summarized in Table 3. Note that these calculations correspond to the high pressure limit.

In the case of 1H isomer the elimination of N_2 is a two-step process which proceeds through the ring-opening reaction with formation of an azide (1AZ, Scheme 5 and Figure 5). As a matter of fact, there are two rotamers of the azide 1AZ undergoing decomposition to different products: carbodiimide and isodiaziridine. The details of the 1AZ decomposition are presented in the

Table 3. Arrhenius Parameters of the Rate Constants of 1H, 2H, 14H, and 5H Decomposition Reactions (1–7)

reaction	rate constant	$\log A, \text{s}^{-1}$	$E_a, \text{kcal/mol}$
1H-TZ \rightarrow 1AZ	k_{1a}	13.72	29.2
1AZ \rightarrow 1H-TZ	k_{-1a}	12.35	14.8
1AZ \rightarrow $\text{NH}=\text{C}=\text{NH} + \text{N}_2$	k_{1b}	14.52	28.4
1H-TZ \rightarrow $\text{NH}=\text{C}=\text{NH} + \text{N}_2$	$k_{1\text{eff}}$	15.88	42.7
1H-TZ \rightarrow HCN + HN_3	k_2	14.79	49.8
2H-TZ \rightarrow $\text{CH}=\text{N}=\text{NH} + \text{N}_2$	k_3	14.78	41.1
2H-TZ \rightarrow HCN + HN_3	k_4	14.64	58.2
14H-TZ \rightarrow $\text{NH}=\text{C}=\text{NH} + \text{N}_2$	k_5	14.85	13.9
14H-TZ \rightarrow HNC + HN_3	k_6	15.43	42.1
5H-TZ \rightarrow $\text{CH}_2=\text{N}_2 + \text{N}_2$	k_7	13.59	2.7

Scheme 5



Supporting Information (Figure S1 and a discussion therein). Note that this decomposition closely resembles the Curtius rearrangement of carbonyl azides.^{81,82} A similar concerted process is also typical of the thermal decomposition of 5-aminotetrazole.^{73,83} Figure 5 displays only one channel of 1AZ decomposition as the second reaction leading to formation of isodiaziridine has a much higher barrier (Supporting Information, Figure S1). Thus, the computations do not support the formation of the nitrene intermediate (Scheme 2)^{46,47} as well as isodiaziridine⁵¹ proposed before.

The reversion of 1AZ to the starting compound (Scheme 5, k_{-1}) is significantly faster than its decay to carbodiimide and N_2 ($k_{-1a} \gg k_{1b}$, Table 3). Thus, the effective rate constant of N_2 formation reads as $k_{1\text{eff}} \cong (k_{1a}/k_{-1a})k_{1b}$ (Table 3).

In contrast to 1H-TZ, the N_2 elimination from the 2H tautomer is a concerted one-step process (Figure 5). The rate constant of this reaction (k_3) is very close to $k_{1\text{eff}}$, a slight difference in the activation energies is compensated by the difference in the A factors (Table 3).

It is worth mentioning that a stepwise mechanism of the 2H-TZ decomposition has also been proposed (see Scheme 4 and a discussion in the Introduction).⁴⁹ To get deeper insight into this problem, we studied the thermodynamics of corresponding open forms of 2H-TZ and their decomposition reactions (Supporting Information, Figure S2 and a discussion therein). The barriers of these reactions turned out to be noticeably higher than that of the concerted reaction (k_3). Thus, the computations do not support the assumptions about the importance of the 2H-TZ ring-opening reactions.⁴⁹

In the meantime, the two higher enthalpy isomers, viz., 14H and 5H, are kinetically unstable and are prone to very fast thermal decomposition via N_2 elimination (Figure 5 and Table 3, k_5 and k_7). It is seen from Table 3 that the lifetime of the singlet carbene 14H ($\tau = 1/k_5$) even at room temperature is $\sim 10^{-5}$ s. The 5H-TZ isomer is even less stable: the activation barrier of N_2 elimination is calculated to be ~ 2 kcal/mol (Figure 5). At room temperature, this corresponds to a lifetime $\tau \sim 1$ ps. As mentioned in the Introduction, the authors of ref 42 calculated a high barrier of a monomolecular hydrogen

transfer (5H-TZ \rightarrow 1H-TZ, cf. Figure 2) and proposed 5H-TZ to be a detectable species. Our findings do not support this suggestion. However, in principle, 5H-TZ should live long enough to be detected in matrices at cryogenic temperatures (~ 10 K and below).

DISCUSSION

Figure 5 demonstrates that the decomposition of all TZ isomers studied lead preferentially to the formation of N_2 ; the elimination of HN_3 is profoundly slower. The products of primary reactions of TZ were detected in the flash vacuum pyrolysis (FVP) experiments.^{51,52} Maier et al.⁵² applied the matrix isolation technique with IR detection of the products of FVP of TZ at 800 °C. The most intensive bands in the IR spectra were assigned to HCN and HN_3 . Other weak IR bands were attributed to nitrilimine ($HC=N=NH$), carbodiimide ($HN=C=NH$), and their isomers (cyanamide (NH_2CN) and diazomethane (CH_2N_2)). However, it is obvious that the IR-inactive N_2 could not be detected. It should be noted that the N_3 -stretching mode has very high intensity in the IR spectrum, and its detection does not exclude that HN_3 is actually a *minor*, but not the most abundant product. Indeed, according to another experimental technique, viz., photoelectron spectroscopy,⁵¹ the most abundant gas products of FVP of TZ at ~ 830 °C were proposed to be N_2 , NH_2CN , HCN, and CH_2N_2 . The latter compounds are isomers and decomposition products of nitrilimine and carbodiimide. Therefore, results of FVP experiments are in agreement with the data of calculations (Figure 5).

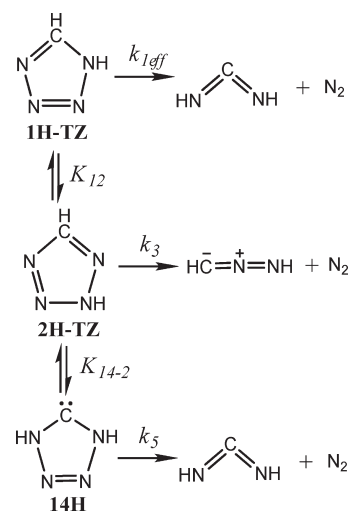
To get insight into the primary stages of TZ thermolysis, one should combine the results given in two previous sections. It is seen from the data of Figure 4 that the activation barriers of the double hydrogen atom transfer in the dimers D11a and D22b are less than 20 kcal/mol. These reactions lead to an interconversion between 1H-TZ and 2H-TZ isomers. These barriers are noticeably lower than those of the monomolecular decomposition of 1H- and 2H-TZ isomers (Figure 5). This implies that the mutual interconversion of 1H and 2H isomers in the dimers is significantly faster than the subsequent monomolecular reactions of N_2 elimination.

However, the monomer–dimer equilibrium is naturally pressure dependent. To study this problem in more detail, we have made several estimations of the typical pressure values (the details of calculations are given in section 2 of the Supporting Information). It was found that at ~ 450 K (recall that the TZ decomposition started near this temperature)⁴⁵ and pressure of TZ higher than 10^{-3} Torr, the 2H- and 1H-TZ isomers are in equilibrium on a time scale of decay. At higher temperatures, the pressure necessary for the establishment of equilibrium on a time scale of thermal decomposition is noticeably higher. For instance, at 600 K the pressure of TZ should be about 10 Torr and higher. Therefore, an equilibrium between the 1H and 2H forms should be taken into account when considering thermolysis of TZ, especially in the melt.

Meanwhile, the barrier of transformation of 1H-TZ into the carbene 14H is about 28 kcal/mol in the H-bonded complex D12b (Figure 4, bottom). The barrier of the reverse reaction D1-14 \rightarrow D12b is quite low (~ 9 kcal/mol). According to our estimations (Supporting Information), the equilibrium between isomers 1H, 2H, and 14H during their decomposition will be maintained at pressures higher than $\sim 10^{-3}$ Torr at 450 K and higher than ~ 10 Torr at 600 K.

As mentioned above, we were unable to localize transition states for the interconversion between 5H-TZ and other TZ tautomers in the H-bonded complexes. In addition, the monomolecular transformation of 1H-TZ to 5H-TZ has a very high barrier (~ 56 kcal/mol, Figure 2). Therefore, we do not consider the equilibrium between 5H-TZ and other tautomers.

Scheme 6



If we take into account only equilibrium between 1H-TZ and 2H-TZ, the effective rate constant of TZ thermal decomposition reads as

$$k_{\text{eff}} = \frac{1}{1 + K_{12}}(k_{1\text{eff}}K_{12} + k_3) \quad (3)$$

where K_{12} is the equilibrium constant:

$$K_{12} = \exp\left(-\frac{\Delta G_{12}}{RT}\right)$$

and ΔG_{12} is the difference of Gibbs free energies of 2H-TZ and 1H-TZ (Figure 5). Using the $k_{1\text{eff}}$ and k_3 values from Table 3, we obtained the Arrhenius parameters of the effective rate constant of TZ thermolysis: $E_a = 41.7$ kcal/mol and $\log A = 15.18$.

If we take into account the equilibrium between the three tautomers 1H-TZ, 2H-TZ, and 14H-TZ (Scheme 6), the effective rate constant of TZ thermolysis can be expressed as

$$k_{\text{eff}} = \frac{1}{1 + K_{12} + K_{14-2}}(k_{1\text{eff}}K_{12} + k_3 + k_5K_{14-2}) \quad (4)$$

where K_{12} is given above and another equilibrium constant is introduced:

$$K_{14-2} = \exp\left(-\frac{\Delta G_{14-2}}{RT}\right)$$

ΔG_{14-2} is the difference of Gibbs free energies of 14H-TZ and 2H-TZ (Figure 5).

It is clear from the data of Figure 5 that the TZ decomposition through the TSS would dominate over other channels. The calculated Arrhenius parameters of the effective rate constant are $E_a = 36.2$ kcal/mol and $\log A = 14.58$. Indeed, once the equilibrium between tautomers (1H-, 2H-, and 14H-TZ) is established, the decomposition of the TZ through the carbene 14H is the most important reaction channel.

As mentioned in the Introduction, the mass loss kinetics of the TZ sample was measured experimentally from the nonisothermal DSC data.^{45,46} The activation energy and the preexponential factor calculated using different approaches varied from 36.5 to 42.6 kcal/mol and from $\log A \approx 14.4$ to $\log A \approx 17.3$.⁴⁵ The

results of our calculations fall into these ranges and perfectly agree with the lowest values (36.5 kcal/mol and $\log A \approx 14.4$).

However, it is more convenient to use isothermal experimental kinetics⁴⁹ for comparison with calculations. As mentioned in the Introduction, activation energy of about 33 kcal/mol was obtained for TZ thermolysis in both the gas phase and nitrobenzene solution.⁴⁹ A slightly higher value of $E_a \approx 37$ kcal/mol was measured for the thermal decomposition in the melt. Again, the computed value of activation energy is in good agreement with experiment.

Recently, da Silva and Bozzelli analyzed the decomposition of 1H and 2H tautomers of TZ.⁵⁵ Using the G3B3 activation barriers and assuming the equal population of 1H and 2H forms, they predicted the Arrhenius parameters of the effective rate constant to be $E_a = 37.8$ kcal/mol and $\log A = 14.79$. However, the corresponding activation energy calculated using very accurate W1 barriers is about 4 kcal/mol higher. Thus, the reason for the agreement of the effective parameters calculated by da Silva and Bozzelli with experiments is the underestimation by G3B3 procedure of the reaction barriers for the decomposition of 1H and 2H tautomers.

As mentioned above, we did not consider decomposition of 5H-TZ in Scheme 6. A comparison of calculations with the experimental data also supports this assumption. If we propose that this tautomer is also in equilibrium with 1H-, 2H-, and 14H-TZ, the decomposition of this species would dominate over all the channels of Scheme 6. The effective activation energy in this case would be about 25 kcal/mol (Figure 5, bottom). This is significantly lower than the ~ 35 –40 kcal/mol observed experimentally.^{45,46,49}

Therefore, the computations allowed clarification of the mechanism and exclusion of some contradictory assumptions of the key reactions and intermediates of TZ thermolysis proposed before.^{46,47,49,51} It should be noted that the mutual interconversion of the TZ tautomers through the concerted double H-transfer in hydrogen-bonded complexes has been introduced for the first time. Moreover, the participation of the carbene isomer 14H in the decomposition of TZ has never been considered previously. On the contrary, according to our computations the values of the effective Arrhenius parameters (E_a and $\log A$) are dominated by the decomposition of this isomer. If we neglect this reaction, the rate of TZ decomposition would be underestimated. Thus, the use of very high level quantum chemical calculations and inclusion of new reactions in the reaction scheme leads to a good agreement between the calculated and experimental Arrhenius parameters of TZ thermolysis.

■ ASSOCIATED CONTENT

Supporting Information. PES for the reactions of the open forms of 1H-TZ and 2H-TZ, estimations of typical pressure values, complete ref 63, optimized geometries of all compounds under study. This material is available free of charge via the Internet at <http://pubs.acs.org>.

■ AUTHOR INFORMATION

Corresponding Author

*E-mail: vitaly.kiselev@kinetics.nsc.ru.

■ ACKNOWLEDGMENT

Support of this work by the Siberian and the Ohio Supercomputer Centers is gratefully acknowledged. V.G.K. also appreciates the support of this work by the Russian Ministry of

Education and Science (Project NK-187P6, Contract No. P1475) and SB RAS (Lavrentiev grant programme).

■ REFERENCES

- (1) Pagoria, P. F.; Lee, G. S.; Mitchell, A. R.; Schmidt, R. D. *Thermochim. Acta* **2002**, *384*, 187.
- (2) Singh, R. P.; Verma, R. D.; Meshri, D. T.; Shreeve, J. M. *Angew. Chem., Int. Ed.* **2006**, *45*, 3584.
- (3) Singh, R. P.; Gao, H.; Meshri, D. T.; Shreeve, J. M. *Struct. Bonding (Berlin)* **2007**, *125*, 35.
- (4) Klapotke, T. M. *Struct. Bonding (Berlin)* **2007**, *125*, 85.
- (5) Steinhäuser, G.; Klapotke, T. M. *Angew. Chem., Int. Ed.* **2008**, *47*, 3330.
- (6) Huynh, M. H. V.; Hiskey, M. A.; Meyer, T. J.; Wetzler, M. *Proc. Natl. Acad. Sci. U.S.A.* **2006**, *103*, 5409.
- (7) Lesnikovich, A. I.; Sviridov, V. V.; Printsev, G. V.; Ivashkevich, O. A.; Gaponik, P. N. *Nature* **1986**, *323*, 706.
- (8) Lesnikovich, A. I.; Printsev, G. V.; Ivashkevich, O. A.; Lyutsko, V. A.; Kovalenko, K. K. *Combust., Explos. Shock Waves* **1987**, *24*, 549.
- (9) Ivashkevich, O. A.; Krasitsky, V. A.; Lesnikovich, A. I.; Astashinsky, V. M.; Kostyukevich, E. A.; Khusid, B. M.; Mansurov, V. A. *Combust. Flame* **1997**, *110*, 113.
- (10) Hammerl, A.; Klapotke, T. M.; Mayer, P.; Weigand, J. J. *Propellants, Explos., Pyrotech.* **2005**, *30*, 17.
- (11) Huynh, M. H. V.; Coburn, M. D.; Meyer, T. J.; Wetzler, M. *Proc. Natl. Acad. Sci. U.S.A.* **2006**, *103*, 10322.
- (12) Klapotke, T. M.; Stein, M.; Stierstorfer, J. Z. *Anorg. Allg. Chem.* **2008**, *634*, 1711.
- (13) Klapotke, T. M.; Sabate, C. M. *Eur. J. Inorg. Chem.* **2008**, 5350.
- (14) Klapotke, T. M.; Sabate, C. M. *Chem. Mater.* **2008**, *20*, 3629.
- (15) Klapotke, T. M.; Mayer, P.; Sabate, C. M.; Welch, J. M.; Wiegand, N. *Inorg. Chem.* **2008**, *47*, 6014.
- (16) Joo, Y.-H.; Shreeve, J. M. *Angew. Chem., Int. Ed.* **2009**, *48*, 564.
- (17) Karaghiosoff, K.; Klapotke, T. M.; Sabate, C. M. *Chem.—Eur. J.* **2009**, *15*, 1164.
- (18) Klapotke, T. M.; Stierstorfer, J. J. *Am. Chem. Soc.* **2009**, *131*, 1122.
- (19) Klapotke, T. M.; Sabate, C. M.; Stierstorfer, J. *New J. Chem.* **2009**, *33*, 136.
- (20) Guo, Y.; Tao, G. H.; Zeng, Z.; Gao, H. X.; Parrish, D. A.; Shreeve, J. M. *Chem.—Eur. J.* **2010**, *16*, 3753.
- (21) Moore, D. S.; Robinson, S. D. *Adv. Inorg. Chem.* **1988**, *32*, 171.
- (22) Zhang, X. M. *Coord. Chem. Rev.* **2005**, *249*, 1201.
- (23) Gaponik, P. N.; Voitekhovich, S. V.; Ivashkevich, O. A. *Russ. Chem. Rev.* **2006**, *75*, 569.
- (24) Patani, G. A.; LaVoie, E. J. *Chem. Rev.* **1996**, *96*, 3147.
- (25) Herr, R. J. *Bioorg. Med. Chem.* **2002**, *10*, 3379.
- (26) Katritzky, A. R.; Lagowski, J. M. *Adv. Heterocycl. Chem.* **1963**, *2*, 27.
- (27) Butler, R. N. *Adv. Heterocycl. Chem.* **1977**, *21*, 323.
- (28) Butler, R. N. Tetrazoles. In *Comprehensive Heterocyclic Chemistry II*; Katritzky, A. R., Rees, C. W., Scriven, E. F. V., Eds.; Pergamon Press: New York, 1997; Vol. 4, p 621.
- (29) Trifonov, R. E.; Ostrovskii, V. A. *Russ. J. Org. Chem.* **2006**, *42*, 1585.
- (30) Ostrovskii, V. A.; Koldobskii, G. I.; Trifonov, R. E. Tetrazoles. In *Comprehensive Heterocyclic Chemistry III*; Katritzky, A. R., Ramsden, C. A., Scriven, E. F. V., Taylor, R. J. K., Eds.; Elsevier: Oxford, Tokyo, 2008; Vol. 6, p 257.
- (31) Otting, W. *Chem. Ber.* **1956**, *89*, 2887.
- (32) Kozyro, A. A.; Simirskii, V. V.; Krasulin, A. P.; Sevruck, V. M.; Kabo, G. Y.; Frenkel, M. L.; Gaponik, P. N.; Grigorev, Y. V. *Russ. J. Chem. Phys.* **1990**, *64*, 348; *Zh. Fiz. Khim.* **1990**, *64*, 656.
- (33) Kabo, G. J.; Kozyro, A. A.; Krasulin, A. P.; Sevruck, V. M.; Ivashkevich, L. S. *J. Chem. Thermodyn.* **1993**, *25*, 485.
- (34) Goddard, R.; Heinemann, O.; Kruger, C. *Acta Crystallogr., Sect. C* **1997**, *53*, 590.

- (35) Krugh, W. D.; Gold, L. P. *J. Mol. Spectrosc.* **1974**, *49*, 423.
- (36) Palmer, M. H.; Simpson, I.; Wheeler, J. R. *Z. Naturforsch. A* **1981**, *36*, 1246.
- (37) Razynska, A.; Tempczyk, A.; Malinski, E.; Szafranek, J.; Grzonka, Z.; Hermann, P. *J. Chem. Soc. Perkin Trans. 2* **1983**, 379.
- (38) Bugalho, S. C. S.; Macoas, E. M. S.; Cristiano, M. L. S.; Fausto, R. *Phys. Chem. Chem. Phys.* **2001**, *3*, 3541.
- (39) Moore, D. W.; Whittaker, A. G. *J. Am. Chem. Soc.* **1960**, *82*, 5007.
- (40) Elguero, J.; Marzin, C.; Roberts, J. D. *J. Org. Chem.* **1974**, *39*, 357.
- (41) Wofford, D. S.; Forkey, D. M.; Russell, J. G. *J. Org. Chem.* **1982**, *47*, 5132.
- (42) Wong, M. W.; Leung-Toung, R.; Wentrup, C. *J. Am. Chem. Soc.* **1993**, *115*, 2465.
- (43) Balabin, R. M. *J. Chem. Phys.* **2009**, *131*, 154307.
- (44) Mazurek, A. P.; Sadleir-Sosnowska, N. *Chem. Phys. Lett.* **2000**, *330*, 212.
- (45) Lesnikovich, A. I.; Ivashkevich, O. A.; Lyutsko, V. A.; Printsev, G. V.; Kovalenko, K. K.; Gaponik, P. N.; Levchik, S. V. *Thermochim. Acta* **1989**, *145*, 195.
- (46) Vyazovkin, S. V.; Lesnikovich, A. I.; Lyutsko, V. A. *Thermochim. Acta* **1990**, *165*, 17.
- (47) Lesnikovich, A. I.; Ivashkevich, O. A.; Printsev, G. V.; Gaponik, P. N.; Levchik, S. V. *Thermochim. Acta* **1990**, *171*, 207.
- (48) Lesnikovich, A. I.; Levchik, S. V.; Balabanovich, A. I.; Ivashkevich, O. A.; Gaponik, P. N. *Thermochim. Acta* **1992**, *200*, 427.
- (49) Prokudin, V. G.; Poplavsky, V. S.; Ostrovskii, V. A. *Russ. Chem. Bull.* **1996**, *45*, 2101.
- (50) Prokudin, V. G.; Poplavsky, V. S.; Ostrovskii, V. A. *Russ. Chem. Bull.* **1996**, *45*, 2094.
- (51) Guimon, C.; Khayar, S.; Gracian, F.; Begtrup, M.; Pfister-Guillouzo, G. *Chem. Phys.* **1989**, *138*, 157.
- (52) Maier, G.; Eckwert, J.; Bothur, A.; Reisenauer, H. P.; Schmidt, C. *Liebigs. Ann.* **1996**, 1041.
- (53) Sinditskii, V. P.; Egorshv, V. Y.; Fogelzang, A. E.; Serushkin, V. V.; Kolesov, V. I. *Chem. Phys. Rep.* **2000**, *18*, 1569; *Khim. Fiz.* **1999**, *18* (8), 87–94.
- (54) Kawaguchi, S.; Kumasaki, M.; Wada, Y.; Arai, M.; Tamura, M. *Kayaku Gakkaishi* **2001**, *62*, 16.
- (55) da Silva, G.; Bozzelli, J. W. *J. Org. Chem.* **2008**, *73*, 1343.
- (56) Martin, J. M. L.; de Oliveira, G. *J. Chem. Phys.* **1999**, *111*, 1843.
- (57) Wood, G. P. F.; Radom, L.; Petersson, G. A.; Barnes, E. C.; Frisch, M. J.; Montgomery, J. A. *J. Chem. Phys.* **2006**, *125*, 094106.
- (58) Barnes, E. C.; Petersson, G. A.; Montgomery, J. A.; Frisch, M. J.; Martin, J. M. L. *J. Chem. Theory Comput.* **2009**, *5*, 2687.
- (59) Baboul, A. G.; Curtiss, L. A.; Redfern, P. C.; Raghavachari, K. *J. Chem. Phys.* **1999**, *110*, 7650.
- (60) Curtiss, L. A.; Raghavachari, K.; Redfern, P. C.; Pople, J. A. *J. Chem. Phys.* **1997**, *106*, 1063.
- (61) Chase, M. W. NIST-JANAF Thermochemical Tables, 4th ed. *J. Phys. Chem. Ref. Data, Monogr.* **1998**, *9* (Suppl. 1), 1.
- (62) Pitzer, K. S.; Gwinn, W. D. *J. Chem. Phys.* **1942**, *10*, 428.
- (63) Full citation of the Gaussian 09 code appears in the Supporting Information.
- (64) Lee, T. J.; Taylor, P. R. *Int. J. Quantum Chem.* **1989**, *S23*, 199.
- (65) McEwan, W. S.; Rigg, M. W. *J. Am. Chem. Soc.* **1951**, *73*, 4725.
- (66) Pedley, J. B. *Thermochemical Data and Structures of Organic Compounds*; Thermodynamic Research Center: College Station, TX, 1994; Vol. 1.
- (67) Balepin, A. A.; Lebedev, V. P.; Miroshnichenko, E. A.; Kolodskii, G. I.; Ostrovskii, V. A.; Larionov, B. P.; Gidaspov, B. V.; Lebedev, Y. A. *Svoistva Veshchestv Str. Mol.* **1977**, 93.
- (68) NIST Chemistry WebBook, NIST Standard Reference Database 69; Linstrom, P. J., Mallard, W. G., Eds.; National Institute of Standards and Technology, Gaithersburg, MD June 2005; <http://webbook.nist.gov/chemistry/>.
- (69) Kiselev, V. G.; Gritsan, N. P. *J. Phys. Chem. A* **2008**, *112*, 4458.
- (70) Williams, M. M.; McEwan, W. S.; Henry, R. A. *J. Phys. Chem.* **1957**, *61*, 261.
- (71) Gutowski, K. E.; Rogers, R. D.; Dixon, D. A. *J. Phys. Chem. A* **2006**, *110*, 11890.
- (72) da Silva, G.; Moore, E. E.; Bozzelli, J. W. *J. Phys. Chem. A* **2006**, *110*, 13979.
- (73) Kiselev, V. G.; Gritsan, N. P. *J. Phys. Chem. A* **2009**, *113*, 3677.
- (74) Lee, M. T.; Hu, C. H. *Organometallics* **2004**, *23*, 976.
- (75) Harmony, M. D.; Laurie, V. W.; Kuczkowski, R. L.; Schwendeman, R. H.; Ramsay, D. A.; Lovas, F. J.; Lafferty, W. J.; Maki, A. G. *J. Phys. Chem. Ref. Data* **1979**, *8*, 619.
- (76) Demaison, J.; Hegelund, F.; Burger, H. *J. Mol. Struct.* **1997**, *413*, 447.
- (77) Kohata, K.; Fukuyama, T.; Kuchitsu, K. *J. Phys. Chem.* **1982**, *86*, 602.
- (78) Bader, R. F. W. *Atoms in Molecules: A Quantum Theory*; Oxford University Press: Oxford, 1990.
- (79) Matta, C. F.; Boyd, R. J., Eds.; *The Quantum Theory of Atoms in Molecules*; Wiley-VCH: Weinheim, 2007.
- (80) Reed, A. E.; Curtiss, L. A.; Weinhold, F. *Chem. Rev.* **1988**, *88*, 899.
- (81) Pritchina, E. A.; Gritsan, N. P.; Maltsev, A.; Bally, T.; Autrey, T.; Liu, Y. L.; Wang, Y. H.; Toscano, J. P. *J. Phys. Chem. Chem. Phys.* **2003**, *5*, 1010.
- (82) Liu, J.; Mandel, S.; Hadad, C. M.; Platz, M. S. *J. Org. Chem.* **2004**, *69*, 8583.
- (83) Paul, K. W.; Hurley, M. M.; Irikura, K. K. *J. Phys. Chem. A* **2009**, *113*, 2483.